

## Infrared ATR Measurements at Low Temperatures. An Apparatus and the Absorption Intensities of Crystalline Benzene and Carbon Disulfide

Haruka YAMADA\* and Masao SAHEKI

Department of Chemistry, Kwansei Gakuin University, Nishinomiya 662

(Received May 17, 1982)

An infrared ATR apparatus for use at low temperatures was constructed for the determination of the optical constants and absorption intensities of crystalline samples. The ATR spectra of benzene and carbon disulfide polycrystals were measured with two different incident angles. The optical constants and then the absorption intensities were accurately obtained for the fundamental bands from these ATR spectra. Experiments for transmission spectra were also carried out with an improved absorption cell at low temperatures, confirming the present ATR results. A comparison of the intensities in different phases was made for the  $\nu_{18}$ ,  $\nu_{19}$ ,  $\nu_{20}$ , and  $\nu_{11}$  fundamental bands of benzene and the  $\nu_3$  band of carbon disulfide.

Studies of infrared intensities have recently attracted revived interest from both theoretical and experimental points of view.<sup>1–4)</sup> Infrared intensities on solids had been studied considerably in the 1960s by measuring the absorption spectra of polycrystalline molecular crystals at low temperatures and by comparing their intensities with those of free molecules. They were discussed in connection with the intermolecular interactions and the field effects.<sup>5–13)</sup> However, the observed intensities included considerable errors caused by ambiguity in the determination of the sample thickness, because the thicknesses were determined by measuring the interference fringes observed when the samples were sublimed from the gases onto a cold window.

We first applied the ATR method to a naphthalene single crystal<sup>14)</sup> in 1971 and succeeded in obtaining the absolute absorption intensities of the fundamental bands. On the basis of the results thus obtained we discussed the deviation from the oriented gas model. Fortunately, naphthalene was a crystal at room temperature and was so soft that good optical contact between naphthalene and an ATR element might be easily made. By the ATR method we could also obtain the infrared intensities for the charge-transfer complexes in a solid.<sup>15)</sup> However, molecular crystals consisting of small molecules, which are convenient for theoretical analysis, are usually liquid or gas at room temperature. If the ATR method can be applied at low temperatures, accurate absorption intensities can be obtained for such crystals. In the present study we have tried to construct an ATR apparatus at low temperatures. With the apparatus, the ATR spectra of polycrystalline benzene and carbon disulfide have been measured.

### ATR Experiments

**Apparatus.** **ATR Cell:** A low-temperature cell, with a hemicylinder (ATR element) of KRS-5 (10 mm radius and 30 mm in height), is shown in Fig. 1. A photograph of the sample part is given in Fig. 1-b. It is made of Pyrex glass (except for the sample part A) and consists of two parts: a cooling part for the ATR element and a sample-spraying part. The outer vessel has two windows, attached with Q wax, whose faces make a right angle. The hemicylinder, H, is supported by a copper holder A and can be cooled down to the temperature of the coolant in E through the connection of Kovar and copper. To make good thermal

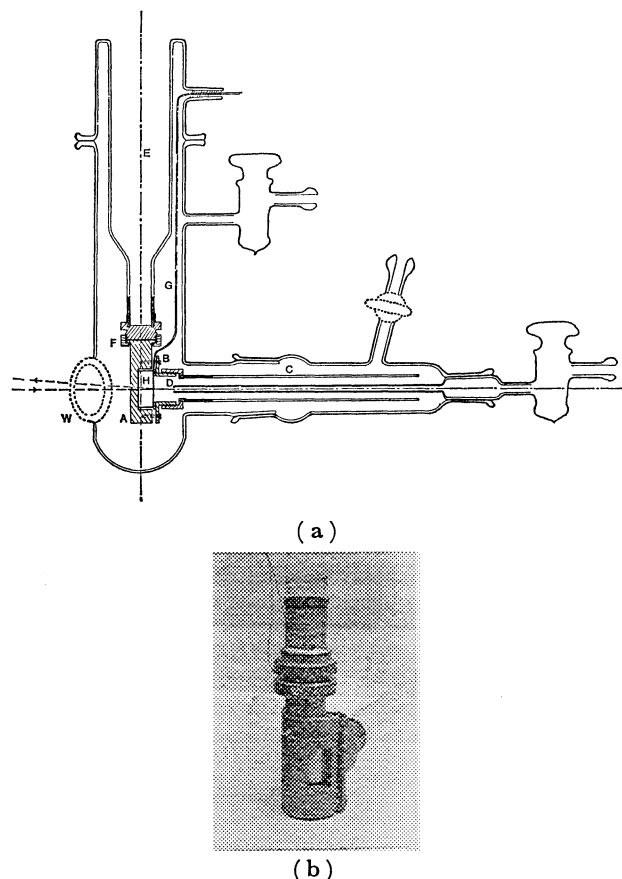


Fig. 1. ATR cell at low temperatures.

contact between A and H, an indium spacer was used. When E was filled with liquid N<sub>2</sub>, the center of H (at the reflecting surface) was cooled to *ca.* 100 K. Sample vapor is directly sublimed onto the reflective surface of H (right side) through the nozzle, D, so that good contact between the ATR element and the sample may be attained. The nozzle is covered with a long glass tube (150 mm) to avoid the condensation of the sample on the back side, that is, on the cylindrical surface of H. The connection B is also made of copper and is equipped with screws. The incident light irradiates H (through the hole of A) and reflects at the interface between H and the deposited sample. By connecting the cell to a vacuum line, it can be evacuated to 10<sup>−4</sup>–10<sup>−6</sup> Torr (1 Torr = 133.322 Pa).

**Optical System:** The optical system for the low-temperature ATR apparatus is shown in Fig. 2. A light source

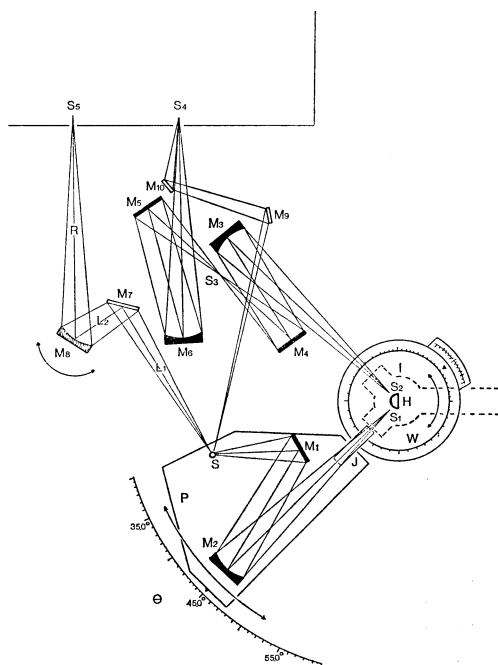


Fig. 2. Optical system.

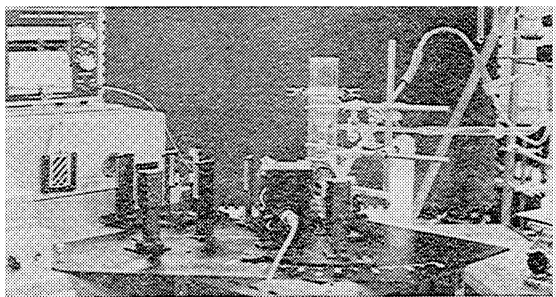


Fig. 3. Uncovered ATR apparatus constructed.

S, a plane mirror  $M_1$ , and a concave mirror  $M_2$  ( $R=340$  mm) are fixed on a plate P, which can move around the ATR cell as it rotates. The ATR cell described above is fixed by clamps on a circular table, W, so that the rotating axis of W may coincide with the cylindrical axis of H. By rotating the circular table, the ATR cell can be rotated around the vertical axis, that is, the cylindrical axis. Connecting P and W with a bar J, P, and W move simultaneously around the same axis. W has an angle graduation marked in degrees with a vernier, so that the incident angle can be known to an accuracy of one minute. The light beam is first focussed on  $S_1$  in front of the cylindrical surface of H, passes through the hemicylinder H as a parallel beam, and is then refocussed on  $S_2$ . Afterwards the light beam is focussed on  $S_3$  and  $S_4$  (the entrance of a monochromator) by concave mirrors,  $M_3$  ( $R=340$  mm) and  $M_6$  ( $R=340$  mm). The mirrors ( $M_3$ ,  $M_4$ ,  $M_5$ , and  $M_6$ ) in Fig. 3 are all fixed.

The reference beam from the light source S is focussed on  $S_5$  by  $M_8$  ( $R=340$  mm), where  $L_1+L_2=R$  (340 mm). A concave mirror  $M_9$  is fixed on its position and can be rotated around the vertical axis;  $M_7$  is approximately placed so as to satisfy:  $L_1+L_2=R$  (340 mm).

Two plane mirrors are used for the correction of the zero line (reflectivity zero) so as to introduce extra light (from S) on  $S_4$ .  $M_9$  and  $M_{10}$  can move and rotate. The angle of incidence can be chosen in the region of  $33-59^\circ$ , making

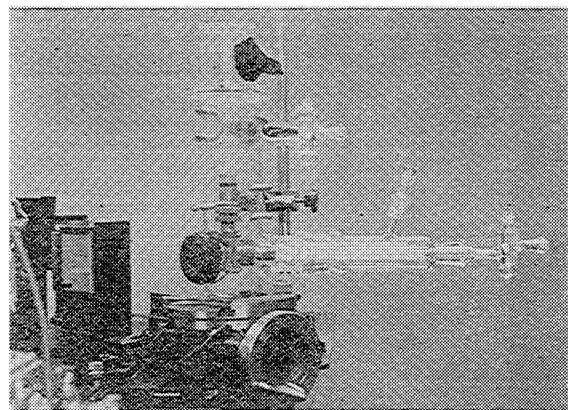


Fig. 4. The ATR cell on the circular table.

a right angle with the cylindrical surface of H.

For the ATR measurements, the optical system can be covered by using plastic sheets and plates; it is blown by dried air to eliminate atmospheric  $H_2O$  and  $CO_2$ .

**Measurements of ATR Spectra.** The uncovered apparatus constructed is shown in Fig. 3. It is connected to a JASCO 402-G spectrophotometer by replacing its source and sample parts, while the cell is connected to a vacuum line.

Figure 4 shows the side view of the low-temperature ATR cell on the circular table. The cell can rotate when the handle is operated.

We first set the angle of incidence at  $45^\circ$ , as is shown in Fig. 2; that is, by connecting W with P the cell direction is set so that the mark (incident angle) on P points to  $45^\circ$  on the base. For any other incident angle, we rotate W with P until the mark on P points to the desired angle  $\theta$ ; then we fix P on the base and disconnect P from W. Next, we rotate the cell, only W, in the opposite direction as much as a half of the angle just moved,  $|\theta-45^\circ|/2$ , and then fix the cell at that position.

**Sampling.** After the apparatus is set as has been described above, the ATR cell is evacuated to  $10^{-4}$ – $10^{-6}$  Torr, and then H is cooled by filling E with a coolant. Sample vapor is sprayed from the nozzle D onto the reflecting surface of H through a needle valve. A uniform film (more than  $20\ \mu\text{m}$  in thickness) can be prepared by controlling the speed of sublimation and the vapor pressure. Samples which are solid at room temperature can also be measured with the apparatus when the samples make optical contact with the ATR element, as in the cases of naphthalene<sup>14)</sup> and iodoform.<sup>16)</sup>

**$R_s$  Measurements.** The polarized ATR spectra of the samples at about 100 K are measured with an AgCl polarizer placed in front of the thermocouple detector. The reflectivity,  $R_s$  (electric vector perpendicular to the incident plane), is measured with two different incident angles,  $\theta_1$  and  $\theta_2$ . The monochromator and the ATR attachment were blown out by dried air passed through molecular sieves.

**Background and Zero Line.** The background is determined by recording  $R_s$  for each incident angle without a sample at that temperature. The zero line of  $R_s$  (reflectivity zero) can be recorded when a shutter is placed in front of the ATR cell with the sample. The true zero curve lowers in the region where the sample absorbs.<sup>21)</sup> To record such a fluctuation, the level of the sample beam has to be kept a little higher than that of the reference by introducing additive energy using  $M_9$  and  $M_{10}$ .

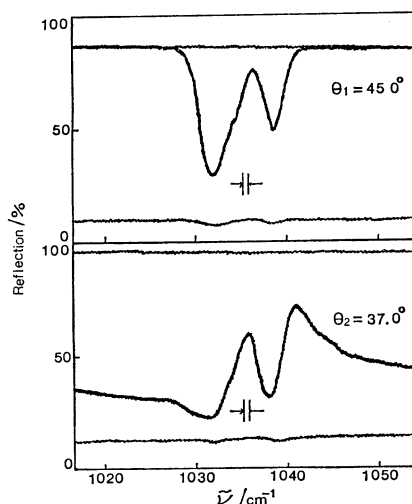


Fig. 5. Apparent  $R_s$  curves of the  $\nu_{20}$  band of polycrystalline benzene with the background and the zero lines at 88 K.

$\rightarrow||\leftarrow$  shows spectral slit width.

### Determination of Optical Constants and Absorption Intensities

The optical constants, refractive index  $n$ , and attenuation index  $k$  can be obtained from the observed ATR spectra.  $n$  and  $k$  are calculated from the reflectivities, ( $R_s$ )'s measured at two different incident angles,  $\theta_1$  and  $\theta_2$ , by the use of polarized light whose electric vectors vibrate perpendicularly to the incident plane. The method used is essentially the same as that previously reported,<sup>14)</sup> namely, the method by Fahrenfort and Visser,<sup>17)</sup> with some modifications suggested by Hansen.<sup>18)</sup>

The computations were performed on a FACOM 270-38 computer. The refractive indices of KRS-5 at 100 K were obtained by correcting the values<sup>19)</sup> for the temperature coefficient. The calculated  $n$ ,  $k$ , and Lambert's  $\alpha = 4\pi nk/\lambda$  values were plotted *vs.* the wave number with a X-Y plotter.

The absorption intensity,  $A$ , is given by:

$$B = \frac{1}{\rho} \int_{\text{band}} \alpha d\tilde{\nu},$$

$$A = \lim_{\Delta s_{1/2} \rightarrow 0} B,$$

where  $\rho$  is the density of the sample crystal and  $\Delta s_{1/2}$ , the spectral slit width. The integration was taken over a region three times as wide as the half-width of the band.

### Benzene Crystal

**ATR Measurements.** Crystalline benzene films were prepared at 88 K by subliming the vapor onto the reflecting surface of the ATR element by a technique similar to that used for transmission measurements.<sup>5,7)</sup> To obtain uniform films, the vapor was deposited as slowly as possible through a needle valve (Edwards High Vacuum), and the junction part (con-

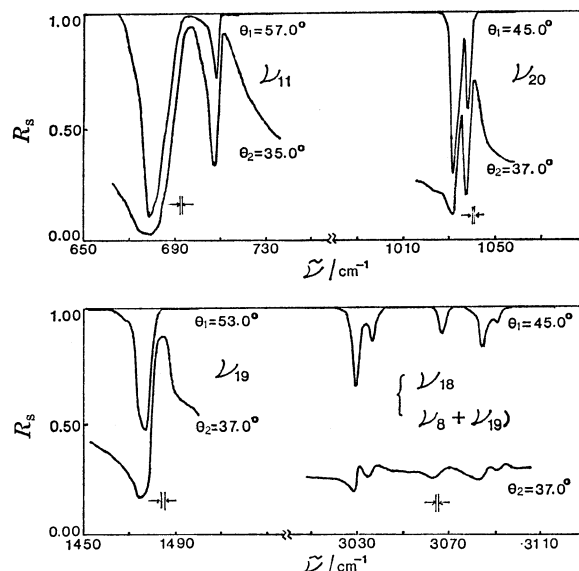


Fig. 6. True  $R_s$  curves for the four fundamental bands of benzene at 88 K.

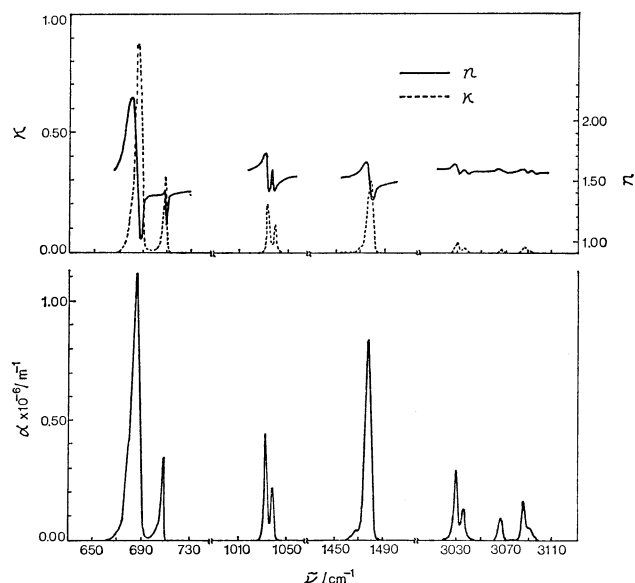


Fig. 7. Optical constants ( $n$ ,  $k$ ) and absorption coefficient ( $\alpha$ ) for polycrystalline benzene at 88 K.

nection of the ATR cell with the spraying tube) was warmed from the outside to prevent vapor deposition in the vicinity of the top of the nozzle. The ATR spectra were measured for the four fundamentals of benzene,  $\nu_{18}$ ,  $\nu_{19}$ ,  $\nu_{20}$ , and  $\nu_{11}$ .

Figure 5 shows the apparent  $R_s$  curves for  $\nu_{20}$  obtained from the ATR measurements with the background and zero lines. For the four fundamentals bands,  $R_s$  curves were obtained as in Fig. 6. The  $n$ ,  $k$ , and  $\alpha$  curves calculated are shown in Fig. 7, which were reproducible for several samples. The average refractive index,  $\bar{n}$ , in the infrared region is obtained as 1.57, which agrees well with the value observed from the polycrystalline benzene at 77 K.<sup>5)</sup> The  $\alpha$  curves obtained coincide well with the transmission curves observed for the stable polycrystalline benzene.<sup>5)</sup>

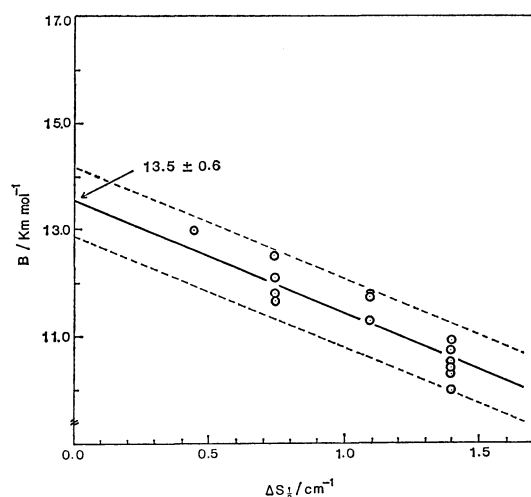


Fig. 8. Plots of  $B$  vs. spectral slit width for the  $\nu_{20}$  band of polycrystalline benzene.

TABLE 1. ABSORPTION INTENSITIES OF BENZENE FUNDAMENTALS IN POLYCRYSTALS ( $1 \text{ km mol}^{-1} = 100 \text{ cm mmol}^{-1}$ )

	$\tilde{\nu}/\text{cm}^{-1}$	$A_{\text{ATR}}$	$A_{\text{Transmission}}^{\text{a)}}$
$\nu_{18}(\text{e}_{1\text{u}})$	3060	$17.2 \pm 2.0$	20.0
$\nu_{19}(\text{e}_{1\text{u}})$	1481	$36.1 \pm 3.0$	37.9
$\nu_{20}(\text{e}_{1\text{u}})$	1036	$13.5 \pm 0.6$	17.6
$\nu_{11}(\text{a}_{2\text{u}})$	685	$81.5 \pm 6.0$	$92.0(80.0)^{\text{b)}}$

a) J. L. Hollenberg and D. A. Dows, *J. Chem. Phys.*, **37**, 1300 (1962). b) D. E. Glover and J. L. Hollenberg, *J. Phys. Chem.*, **73**, 889 (1969).

( $R_s$ )'s could be measured with an error of less than 0.5% for  $\nu_{18}$ ,  $\nu_{19}$ ,  $\nu_{20}$ , and  $\nu_{11}$ , resulting in accuracies of  $\pm 2\%$  for  $n$ ,  $\pm(4-13)\%$  for  $k$ , and  $\pm(4-12)\%$  for  $\alpha$  at the peaks.

The integrated absorption intensities,  $B$ , for the four fundamental bands can be obtained from the  $\alpha$  curves, using  $\rho$  (density)  $= 1.42 \times 10^4 \text{ mol m}^{-3}$ . Since the spectral slit widths,  $\Delta S_{1/2}$ , used were not so small as the half-widths,  $\Delta \tilde{\nu}_{1/2}$ , of the respective bands, corrections for a finite spectral slit-width were needed. For  $\nu_{18}$  and  $\nu_{19}$ , the condition  $(1/3) \Delta \tilde{\nu}_{1/2} > \Delta S_{1/2}$  is satisfied, so  $\Delta \tilde{\nu}_{1/2}$  and  $B$  are almost constant over the spectral slit-widths used, 1.3–1.8  $\text{cm}^{-1}$ ; therefore  $B \approx A$ . On the other hand, the above condition did not

hold for  $\nu_{20}$  and  $\nu_{11}$ . The absolute absorption intensities for  $\nu_{20}$  and  $\nu_{11}$  were then obtained by extrapolating  $B$ 's to  $\Delta S_{1/2} \rightarrow 0$ . The plots of  $B$  vs.  $\Delta S_{1/2}$  are shown for  $\nu_{20}$  in Fig. 8.

In Table 1 the absolute absorption intensities,  $A$ , obtained from the ATR measurements are given for the fundamental bands, together with the values reported from the transmission measurements. The present ATR values are all smaller than those reported from the transmission measurements. The ratios of the values between ATR and transmission differ from band to band in the 77–95% region. The smaller the intensity value, the smaller the ratio. The values obtained from the ATR measurements are independent of the sample thickness and are certainly more accurate than those reported from the transmission measurements.

**Intensity Changes in Different Phases.** Now that we have obtained reliable intensities in solid benzene, we can proceed to compare the values in different phases. Going from gas to a solid, the intensity of the  $\nu_{18}$  band decreases to about 1/3 of the gaseous value, while that of the  $\nu_{19}$  band increases by three times. The  $\nu_{20}$  band also increases in intensity a little going from gas to a solid. The intensity changes observed, thus, vary with the bands in both direction and amount, and do not depend on the symmetry species to which the vibrational mode belongs. For the  $\nu_{11}$  band, the value in the liquid phase is still uncertain, so at present no appropriate comparison can be made for the  $\nu_{11}$  band.

**Transmission Measurements.** We have succeeded in obtaining the absorption intensities for the benzene polycrystal from the ATR measurements. The present values are smaller by 5–23% than the intensities reported from the transmission measurements. The inaccuracy in obtaining  $A$  from the transmission measurements is mainly caused by the determination of the thickness of the film used. However, it seems probable to improve the transmission experiments, for during the ATR measurements we noticed that the samples were sublimed easily on the cylindrical (back) surface of the ATR element unless quite a long shielding tube was used. Judging from the structure of the cold cell used previously for the transmission measurements, it is supposed that the samples were sublimed onto both sides of the substrate. Therefore, we tried to modify the old cell in the way shown in Fig. 9.

TABLE 2. COMPARISON OF ABSORPTION INTENSITIES OF FUNDAMENTAL BANDS OF BENZENE IN THREE PHASES ( $\text{km mol}^{-1}$ )

	$\tilde{\nu}/\text{cm}^{-1}$	Gas	Liquid		Solid
		Transmission <sup>a)</sup>	ATR <sup>b)</sup>	Transmission <sup>d)</sup>	ATR
$\nu_{18}(\text{e}_{1\text{u}})$	3060	59.8	(48.0) <sup>c)</sup>	44.4	17.2
$\nu_{19}(\text{e}_{1\text{u}})$	1481	13.0	—	19.1	36.1
$\nu_{20}(\text{e}_{1\text{u}})$	1036	8.80	12.9	11.5	13.5
$\nu_{11}(\text{a}_{2\text{u}})$	685	87.8	142	95.4	81.5

a) H. Spedding and D. H. Whiffen, *Proc. R. Soc. London, Ser. A*, **238**, 245 (1956). b) A. C. Gilby, J. Burr, Jr., W. Krueger, and B. Crawford, Jr., *J. Phys. Chem.*, **70**, 1525 (1966). c) G. M. Irons and H. W. Thompson, *Proc. R. Soc. London, Ser. A*, **298**, 160 (1967). d) I. C. Hisatsune and E. S. Jayadevappa, *J. Chem. Phys.*, **32**, 565 (1960).

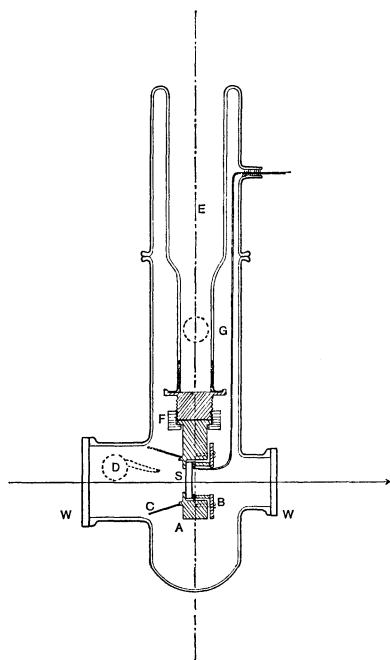


Fig. 9. Improved transmission cell at low temperatures.

A shielding cover, C, made of a thin copper sheet was attached to the copper block, A, with solder around the substrate (KRS-5,  $20 \times 10$  mm). The top of the nozzle, D, had to be inserted into C, and the separation of D from the substrate surface should be 20 mm, so that the sample vapor can be sublimed uniformly onto the front side (and not onto the back surface) of the substrate.

The transmission spectra of polycrystalline thin films of benzene were measured with a modified cold cell attached to the JASCO DS-402G infrared spectrophotometer. The sampling and spectral measurements were the same as those described earlier.<sup>13,14</sup> The thickness of the sample was estimated by counting the interference fringes which were observed by the Hollenberg-Dows method,<sup>5</sup> when the sample vapor was subliming onto the substrate.

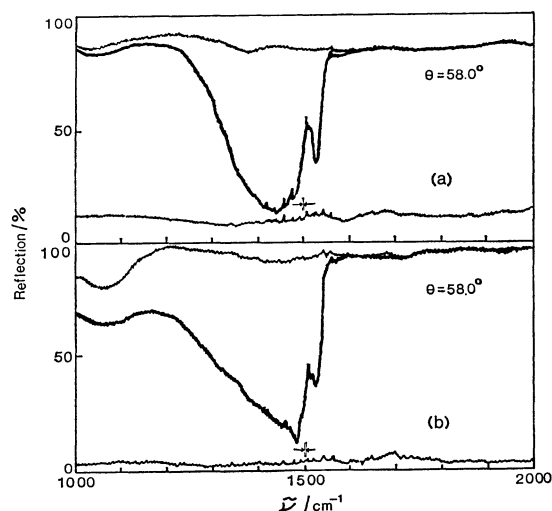
The integrated absorption intensity was calculated by means of:

$$B = \frac{1}{\rho l} \int_{\text{band}} \ln(I_0/I) d\bar{\nu},$$

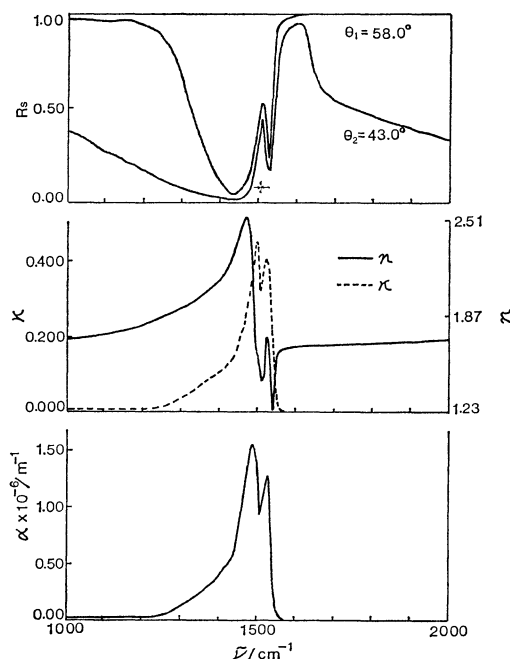
where  $\rho$  is the density and  $l$ , the thickness of the sample crystal. The intensities,  $A$ , corrected for a finite spectral slit width are  $16.3 \pm 1.0$  for  $\nu_{18}$ ,  $31.7$  for  $\nu_{19}$ ,  $14.2 \pm 0.6$  for  $\nu_{20}$ , and  $74.5 \pm 3.5$  for  $\nu_{11}$  in  $\text{km mol}^{-1}$  units; these are rather close to the values obtained from the ATR measurements and seem to justify the present ATR results.

### Carbon Disulfide Crystal

Polycrystalline carbon disulfide was also measured by the ATR method. Because of the high vapor pressure and the low melting point of  $\text{CS}_2$ , especially careful sublimation was carried out in order to obtain uniform and stable polycrystals. If the holder B was colder than the reflecting surface of H, the  $\text{CS}_2$  vapor

Fig. 10. Apparent  $R_s$  curves for sprayed carbon disulfide at 109 K.

(a): Slowly deposited sample, (b): rapidly deposited sample.

Fig. 11.  $R_s$ ,  $n$ ,  $k$ , and  $\alpha$  curves for polycrystalline carbon disulfide at 109 K.

was first condensed onto B, not on H. We inserted, therefore, a Teflon spacer between B and H, so that the temperature of H was kept higher by 20–30 K than that of B.

The ATR spectra were measured for a fundamental band,  $\nu_3$ . When the  $\text{CS}_2$  vapor was sprayed onto H, two kinds of spectra were observed, depending on the spraying speed. The spectra observed with  $\theta = 58^\circ$  and at 109 K are shown in Fig. 10; (a) was obtained with the speed of  $4.6 \times 10^{-4} \text{ mol h}^{-1}$  and (b) with that of  $2.8 \times 10^{-2} \text{ mol h}^{-1}$ . The (a) spectrum is sharper than the (b) spectrum. Comparing these spectra with those observed for the transmission measurements,<sup>7</sup> the (a) spectrum is, seen to be quite similar to the trans-

TABLE 3. ABSORPTION INTENSITIES OF THE  $\nu_3$  BAND OF CS<sub>2</sub> IN THREE PHASES (km mol<sup>-1</sup>)

$\tilde{\nu}/\text{cm}^{-1}$	Gas <sup>a)</sup>	Liquid <sup>a)</sup>	Solid	
			ATR	Transmission <sup>a)</sup>
$\approx 1500$	$567 \pm 10$	$752 \pm 20$	$725 \pm 110$	$800 \pm 140$

a) H. Yamada and W. B. Person, *J. Chem. Phys.*, **40**, 309 (1964).

mission spectrum observed for the stable thin polycrystalline CS<sub>2</sub>, except for a small peak at 1457 cm<sup>-1</sup> observed for the transmission. The small peak at 1457 cm<sup>-1</sup>, assigned to the isotopic molecule, <sup>13</sup>CS<sub>2</sub>, was also observed during the sample sublimation for the thin film, but was obscured for the present thick sample. The peaks at 1530 and 1485 cm<sup>-1</sup> are components of  $\nu_3$  split by the correlation-field effect.<sup>7)</sup> The (b) or a similar spectrum was observed for a worse (not uniform) or unstable crystal.

The optical constants and absorption intensity were determined for the samples which showed the (a) spectrum. The  $R_s$ ,  $n$ ,  $k$ , and  $\alpha$  curves are shown in Fig. 11. The mean refractive index,  $\bar{n}$ , is obtained as 1.80, which is close to the value,  $1.82 \pm 0.05$ , obtained for the polycrystalline CS<sub>2</sub> at *ca.* 80 K.

The absorption intensity,  $A$ , was calculated, to be 725 km mol<sup>-1</sup>, using  $\rho = 2.13 \times 10^4$  mol m<sup>-3</sup> (109 K), estimated from the X-ray structure;<sup>20)</sup> this value is a little smaller than the value obtained from the transmission measurements.<sup>7)</sup> The  $\nu_3$  band is so broad that the correction for the finite spectral slit width is negligible. The  $A$  values are tabulated with the values reported from the transmission measurements. The difference in values between ATR and transmission is rather small for the  $\nu_3$  band of CS<sub>2</sub>. This might be explained as follows: Because of the strength of  $\nu_3$ , extremely thin films were prepared for the transmission measurements. The sublimation time, therefore, was so short that the back-side deposition of CS<sub>2</sub> might not be so serious as for the benzene crystal. Consequently, it seems that the error included in  $A$  was not so serious for the transmission band of  $\nu_3$ . For the CS<sub>2</sub> crystal, the previous results<sup>7)</sup> are confirmed

by the present ATR measurements.

## References

- 1) D. Steele, "Molecular Spectroscopy," ed by R. F. Barrow, D. A. Long, and D. J. Millen, The Chemical Society, London (1978), Vol. 5, p. 106.
- 2) W. B. Person and D. Steele, "Molecular Spectroscopy," ed by R. F. Barrow, D. A. Long, and D. J. Millen, The Chemical Society, London (1974), Vol. 2, p. 357.
- 3) B. Crawford, Jr., T. G. Goplen, and D. Swanson, "Advances in Infrared and Raman Spectroscopy," ed by R. J. H. Clark and R. E. Hester, Heyden, London (1978), Vol. IV, Chap. 2.
- 4) R. N. Jones *et al.*, *Appl. Spectrosc.*, **34**, 638, 691 (1980).
- 5) J. L. Hollenberg and D. A. Dows, *J. Chem. Phys.*, **37**, 1300 (1962).
- 6) G. M. Wieder and D. A. Dows, *J. Chem. Phys.*, **37**, 2990 (1962).
- 7) H. Yamada and W. B. Person, *J. Chem. Phys.*, **40**, 309 (1964).
- 8) H. B. Friedrich and W. B. Person, *J. Chem. Phys.*, **39**, 811 (1963); H. B. Friedrich, H. Yamada, and W. B. Person, *ibid.*, **43**, 418 (1965).
- 9) H. Yamada and W. B. Person, *J. Chem. Phys.*, **41**, 2478 (1964); **43**, 2519 (1965).
- 10) T. L. Brown, *J. Chem. Phys.*, **43**, 2780 (1965).
- 11) D. A. Dows, *Spectrochim. Acta*, **22**, 1479 (1966).
- 12) C. F. Cook, W. B. Person, and L. C. Hall, *Spectrochim. Acta*, **23A**, 1425 (1967).
- 13) A. Kimoto and H. Yamada, *Bull. Chem. Soc. Jpn.*, **41**, 1096 (1968).
- 14) K. Tsuji and H. Yamada, *J. Phys. Chem.*, **76**, 260 (1971).
- 15) M. Saheki and H. Yamada, *Spectrochim. Acta*, **32A**, 1425 (1976).
- 16) K. Tsuji and H. Yamada, *Bull. Chem. Soc. Jpn.*, **41**, 1975 (1968).
- 17) J. Fahrenfort and W. M. Wisser, *Spectrochim. Acta*, **18**, 1103 (1962).
- 18) W. N. Hansen, *Spectrochim. Acta*, **21**, 209 (1965).
- 19) W. S. Rodney and I. H. Malitson, *J. Opt. Soc. Am.*, **46**, 956 (1956).
- 20) N. C. Baenziger and W. L. Duax, *J. Chem. Phys.*, **48**, 2974 (1968).
- 21) H. Yamada, *Jasco Report*, **2**, No. 12, 7 (1965).